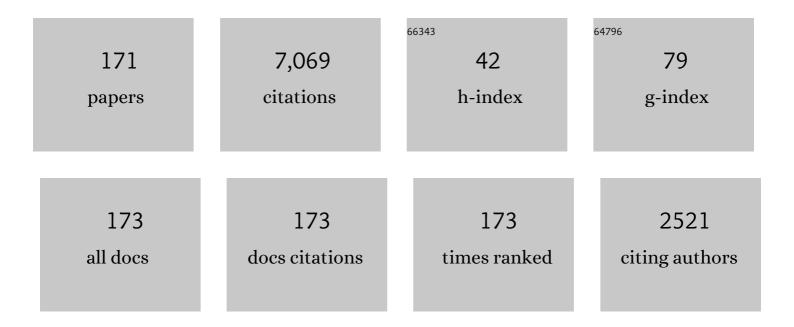
Mariolino De Cecco

List of Publications by Year in descending order

Source: https://exaly.com/author-pdf/7928882/publications.pdf Version: 2024-02-01



#	Article	IF	CITATIONS
1	On the nucleus structure and activity of comet 67P/Churyumov-Gerasimenko. Science, 2015, 347, aaa1044.	12.6	366
2	Dust measurements in the coma of comet 67P/Churyumov-Gerasimenko inbound to the Sun. Science, 2015, 347, aaa3905.	12.6	310
3	OSIRIS – The Scientific Camera System Onboard Rosetta. Space Science Reviews, 2007, 128, 433-506.	8.1	286
4	The morphological diversity of comet 67P/Churyumov-Gerasimenko. Science, 2015, 347, aaa0440.	12.6	259
5	The global shape, density and rotation of Comet 67P/Churyumov-Gerasimenko from preperihelion Rosetta/OSIRIS observations. Icarus, 2016, 277, 257-278.	2.5	252
6	Shape model, reference system definition, and cartographic mapping standards for comet 67P/Churyumov-Gerasimenko – Stereo-photogrammetric analysis of Rosetta/OSIRIS image data. Astronomy and Astrophysics, 2015, 583, A33.	5.1	188
7	Spectrophotometric properties of the nucleus of comet 67P/Churyumov-Gerasimenko from the OSIRIS instrument onboard the ROSETTA spacecraft. Astronomy and Astrophysics, 2015, 583, A30.	5.1	188
8	Images of Asteroid 21 Lutetia: A Remnant Planetesimal from the Early Solar System. Science, 2011, 334, 487-490.	12.6	179
9	Insolation, erosion, and morphology of comet 67P/Churyumov-Gerasimenko. Astronomy and Astrophysics, 2015, 583, A34.	5.1	173
10	The primordial nucleus of comet 67P/Churyumov-Gerasimenko. Astronomy and Astrophysics, 2016, 592, A63.	5.1	159
11	Large heterogeneities in comet 67P as revealed by active pits from sinkhole collapse. Nature, 2015, 523, 63-66.	27.8	158
12	EVOLUTION OF THE DUST SIZE DISTRIBUTION OF COMET 67P/CHURYUMOV–GERASIMENKO FROM 2.2 au TO PERIHELION. Astrophysical Journal, 2016, 821, 19.	4.5	158
13	Regional surface morphology of comet 67P/Churyumov-Gerasimenko from Rosetta/OSIRIS images. Astronomy and Astrophysics, 2015, 583, A26.	5.1	153
14	Redistribution of particles across the nucleus of comet 67P/Churyumov-Gerasimenko. Astronomy and Astrophysics, 2015, 583, A17.	5.1	149
15	Two independent and primitive envelopes of the bilobate nucleus of comet 67P. Nature, 2015, 526, 402-405.	27.8	141
16	E-Type Asteroid (2867) Steins as Imaged by OSIRIS on Board Rosetta. Science, 2010, 327, 190-193.	12.6	120
17	Gravitational slopes, geomorphology, and material strengths of the nucleus of comet 67P/Churyumov-Gerasimenko from OSIRIS observations. Astronomy and Astrophysics, 2015, 583, A32.	5.1	113
18	Summer fireworks on comet 67P. Monthly Notices of the Royal Astronomical Society, 2016, 462, S184-S194.	4.4	112

#	Article	IF	CITATIONS
19	Seasonal mass transfer on the nucleus of comet 67P/Chuyumov–Gerasimenko. Monthly Notices of the Royal Astronomical Society, 2017, 469, S357-S371.	4.4	111
20	Size-frequency distribution of boulders ≥7 m on comet 67P/Churyumov-Gerasimenko. Astronomy and Astrophysics, 2015, 583, A37.	5.1	108
21	The global meter-level shape model of comet 67P/Churyumov-Gerasimenko. Astronomy and Astrophysics, 2017, 607, L1.	5.1	107
22	Are fractured cliffs the source of cometary dust jets? Insights from OSIRIS/Rosetta at 67P/Churyumov-Gerasimenko. Astronomy and Astrophysics, 2016, 587, A14.	5.1	102
23	The pristine interior of comet 67P revealed by the combined Aswan outburst and cliff collapse. Nature Astronomy, 2017, 1, .	10.1	100
24	OSIRIS observations of meter-sized exposures of H ₂ O ice at the surface of 67P/Churyumov-Gerasimenko and interpretation using laboratory experiments. Astronomy and Astrophysics, 2015, 583, A25.	5.1	97
25	Rosetta's comet 67P/Churyumov-Gerasimenko sheds its dusty mantle to reveal its icy nature. Science, 2016, 354, 1566-1570.	12.6	97
26	Regional surface morphology of comet 67P/Churyumov-Gerasimenko from Rosetta/OSIRIS images: The southern hemisphere. Astronomy and Astrophysics, 2016, 593, A110.	5.1	86
27	The rotation state of 67P/Churyumov-Gerasimenko from approach observations with the OSIRIS cameras on Rosetta. Astronomy and Astrophysics, 2014, 569, L2.	5.1	81
28	3D Tracking of Human Motion Using Visual Skeletonization and Stereoscopic Vision. Frontiers in Bioengineering and Biotechnology, 2020, 8, 181.	4.1	81
29	Fractures on comet 67P/Churyumov erasimenko observed by Rosetta/OSIRIS. Geophysical Research Letters, 2015, 42, 5170-5178.	4.0	71
30	Scientific assessment of the quality of OSIRIS images. Astronomy and Astrophysics, 2015, 583, A46.	5.1	67
31	Surface changes on comet 67P/Churyumov-Gerasimenko suggest a more active past. Science, 2017, 355, 1392-1395.	12.6	63
32	67P/Churyumov-Gerasimenko: Activity between March and June 2014 as observed from Rosetta/OSIRIS. Astronomy and Astrophysics, 2015, 573, A62.	5.1	60
33	Temporal morphological changes in the Imhotep region of comet 67P/Churyumov-Gerasimenko. Astronomy and Astrophysics, 2015, 583, A36.	5.1	60
34	The 2016 Feb 19 outburst of comet 67P/CG: an ESA Rosetta multi-instrument study. Monthly Notices of the Royal Astronomical Society, 2016, 462, S220-S234.	4.4	60
35	Geomorphology of the Imhotep region on comet 67P/Churyumov-Gerasimenko from OSIRIS observations. Astronomy and Astrophysics, 2015, 583, A35.	5.1	59
36	Sunset jets observed on comet 67P/Churyumov-Gerasimenko sustained by subsurface thermal lag. Astronomy and Astrophysics, 2016, 586, A7.	5.1	55

#	Article	IF	CITATIONS
37	Comet 67P/Churyumov-Gerasimenko: Constraints on its origin from OSIRIS observations. Astronomy and Astrophysics, 2015, 583, A44.	5.1	53
38	Aswan site on comet 67P/Churyumov-Gerasimenko: Morphology, boulder evolution, and spectrophotometry. Astronomy and Astrophysics, 2016, 592, A69.	5.1	53
39	Acceleration of individual, decimetre-sized aggregates in the lower coma of comet 67P/Churyumov–Gerasimenko. Monthly Notices of the Royal Astronomical Society, 2016, 462, S78-S88.	4.4	52
40	Evidence of sub-surface energy storage in comet 67P from the outburst of 2016 July 03. Monthly Notices of the Royal Astronomical Society, 2017, 469, s606-s625.	4.4	45
41	The scattering phase function of comet 67P/Churyumov–Gerasimenko coma as seen from the Rosetta/OSIRIS instrument. Monthly Notices of the Royal Astronomical Society, 2017, 469, S404-S415.	4.4	44
42	Seasonal erosion and restoration of the dust cover on comet 67P/Churyumov-Gerasimenko as observed by OSIRIS onboard Rosetta. Astronomy and Astrophysics, 2017, 604, A114.	5.1	43
43	Dust mass distribution around comet 67P/Churyumov–Gerasimenko determined via parallax measurements using Rosetta's OSIRIS cameras. Monthly Notices of the Royal Astronomical Society, 2017, 469, S276-S284.	4.4	43
44	Variegation of comet 67P/Churyumov-Gerasimenko in regions showing activity. Astronomy and Astrophysics, 2016, 586, A80.	5.1	43
45	Geomorphology and spectrophotometry of Philae's landing site on comet 67P/Churyumov-Gerasimenko. Astronomy and Astrophysics, 2015, 583, A41.	5.1	41
46	The pebbles/boulders size distributions on Sais: Rosetta's final landing site on comet 67P/Churyumov–Gerasimenko. Monthly Notices of the Royal Astronomical Society, 2017, 469, S636-S645.	4.4	40
47	Tensile strength of 67P/Churyumov–Gerasimenko nucleus material from overhangs. Astronomy and Astrophysics, 2018, 611, A33.	5.1	40
48	Large-scale dust jets in the coma of 67P/Churyumov-Gerasimenko as seen by the OSIRIS instrument onboard Rosetta. Astronomy and Astrophysics, 2015, 583, A9.	5.1	39
49	The dust environment of comet 67P/Churyumov-Gerasimenko from Rosetta OSIRIS and VLT observations in the 4.5 to 2.9 AU heliocentric distance range inbound. Astronomy and Astrophysics, 2016, 587, A155.	5.1	39
50	Thermal modelling of water activity on comet 67P/Churyumov-Gerasimenko with global dust mantle and plural dust-to-ice ratio. Monthly Notices of the Royal Astronomical Society, 2017, 469, S295-S311.	4.4	39
51	CHANGES IN THE PHYSICAL ENVIRONMENT OF THE INNER COMA OF 67P/CHURYUMOV–GERASIMENKO WITH DECREASING HELIOCENTRIC DISTANCE. Astronomical Journal, 2016, 152, 130.	4.7	36
52	Gas outflow and dust transport of comet 67P/Churyumov–Gerasimenko. Monthly Notices of the Royal Astronomical Society, 2016, 462, S533-S546.	4.4	34
53	Observations and analysis of a curved jet in the coma of comet 67P/Churyumov-Gerasimenko. Astronomy and Astrophysics, 2016, 588, L3.	5.1	34
54	Tutorial 14: multisensor data fusion. IEEE Instrumentation and Measurement Magazine, 2008, 11, 24-33.	1.6	33

#	Article	IF	CITATIONS
55	Morphology and dynamics of the jets of comet 67P/Churyumov-Gerasimenko: Early-phase development. Astronomy and Astrophysics, 2015, 583, A11.	5.1	33
56	Constraints on cometary surface evolution derived from a statistical analysis of 67P's topography. Monthly Notices of the Royal Astronomical Society, 2017, 469, S329-S338.	4.4	33
57	Meter-scale thermal contraction crack polygons on the nucleus of comet 67P/Churyumov-Gerasimenko. Icarus, 2018, 301, 173-188.	2.5	33
58	Regional unit definition for the nucleus of comet 67P/Churyumov-Gerasimenko on the SHAP7 model. Planetary and Space Science, 2018, 164, 19-36.	1.7	32
59	Autonomous pallet localization and picking for industrial forklifts: a robust range and look method. Measurement Science and Technology, 2011, 22, 085502.	2.6	30
60	The highly active Anhur–Bes regions in the 67P/Churyumov–Gerasimenko comet: results from OSIRIS/ROSETTA observations. Monthly Notices of the Royal Astronomical Society, 2017, 469, S93-S107.	4.4	30
61	A mini outburst from the nightside of comet 67P/Churyumov-Gerasimenko observed by the OSIRIS camera on Rosetta. Astronomy and Astrophysics, 2016, 596, A89.	5.1	29
62	Information Dynamics of the Brain, Cardiovascular and Respiratory Network during Different Levels of Mental Stress. Entropy, 2019, 21, 275.	2.2	29
63	Observations of Comet 9P/Tempel 1 around the Deep Impact event by the OSIRIS cameras onboard Rosetta. Icarus, 2007, 187, 87-103.	2.5	27
64	Geologic mapping of the Comet 67P/Churyumov–Gerasimenko's Northern hemisphere. Monthly Notices of the Royal Astronomical Society, 2016, 462, S352-S367.	4.4	27
65	The southern hemisphere of 67P/Churyumov-Gerasimenko: Analysis of the preperihelion size-frequency distribution of boulders ≥7 m. Astronomy and Astrophysics, 2016, 592, L2.	5.1	27
66	Rotating dust particles in the coma of comet 67P/Churyumov-Gerasimenko. Astronomy and Astrophysics, 2015, 583, A14.	5.1	26
67	Characterization of the Abydos region through OSIRIS high-resolution images in support of CIVA measurements. Astronomy and Astrophysics, 2016, 585, L1.	5.1	26
68	Decimetre-scaled spectrophotometric properties of the nucleus of comet 67P/Churyumov–Gerasimenko from OSIRIS observations. Monthly Notices of the Royal Astronomical Society, 2016, 462, S287-S303.	4.4	26
69	Dynamic Measurements of Impulses Generated by the Separation of Adhered Bodies under Near-Zero Gravity Conditions. Experimental Mechanics, 2008, 48, 777-787.	2.0	24
70	Long-term survival of surface water ice on comet 67P. Monthly Notices of the Royal Astronomical Society, 2017, 469, S582-S597.	4.4	24
71	Orbital elements of the material surrounding comet 67P/Churyumov-Gerasimenko. Astronomy and Astrophysics, 2015, 583, A16.	5.1	23
72	Sublimation of icy aggregates in the coma of comet 67P/Churyumov–Gerasimenko detected with the OSIRIS cameras on board <i>Rosetta</i> . Monthly Notices of the Royal Astronomical Society, 2016, 462, S57-S66.	4.4	23

#	Article	IF	CITATIONS
73	Geomorphological mapping of comet 67P/Churyumov–Gerasimenko's Southern hemisphere. Monthly Notices of the Royal Astronomical Society, 2016, 462, S573-S592.	4.4	23
74	Investigating the physical properties of outbursts on comet 67P/Churyumov–Gerasimenko. Monthly Notices of the Royal Astronomical Society, 2017, 469, S731-S740.	4.4	23
75	Physical properties and dynamical relation of the circular depressions on comet 67P/Churyumov-Gerasimenko. Astronomy and Astrophysics, 2016, 591, A132.	5.1	22
76	The opposition effect of 67P/Churyumov–Gerasimenko on post-perihelion Rosetta images. Monthly Notices of the Royal Astronomical Society, 2017, 469, S550-S567.	4.4	22
77	A three-dimensional modelling of the layered structure of comet 67P/Churyumov-Gerasimenko. Monthly Notices of the Royal Astronomical Society, 2017, 469, S741-S754.	4.4	22
78	Bilobate comet morphology and internal structure controlled by shear deformation. Nature Geoscience, 2019, 12, 157-162.	12.9	22
79	Automatic graph based spatiotemporal extrinsic calibration of multiple Kinect V2 ToF cameras. Robotics and Autonomous Systems, 2017, 98, 105-125.	5.1	21
80	On deviations from free-radial outflow in the inner coma of comet 67P/Churyumov–Gerasimenko. Icarus, 2018, 311, 1-22.	2.5	21
81	Spectrophotometry of the Khonsu region on the comet 67P/Churyumov–Gerasimenko using OSIRIS instrument images. Monthly Notices of the Royal Astronomical Society, 2016, 462, S274-S286.	4.4	20
82	The phase function and density of the dust observed at comet 67P/Churyumov–Gerasimenko. Monthly Notices of the Royal Astronomical Society, 2018, 476, 2835-2839.	4.4	20
83	Models of Rosetta/OSIRIS 67P Dust Coma Phase Function. Astronomical Journal, 2018, 156, 237.	4.7	20
84	LISA Pathfinder test mass injection in geodesic motion: status of the on-ground testing. Classical and Quantum Gravity, 2009, 26, 094011.	4.0	19
85	Coma morphology of comet 67P controlled by insolation over irregular nucleus. Nature Astronomy, 2018, 2, 562-567.	10.1	19
86	Comparative study of water ice exposures on cometary nuclei using multispectral imaging data. Monthly Notices of the Royal Astronomical Society, 2016, 462, S394-S414.	4.4	18
87	Linking surface morphology, composition, and activity on the nucleus of 67P/Churyumov-Gerasimenko. Astronomy and Astrophysics, 2019, 630, A7.	5.1	18
88	Uncertainty evaluation for complex propagation models by means of the theory of evidence. Measurement Science and Technology, 2008, 19, 055103.	2.6	17
89	Measurement of momentum transfer due to adhesive forces: On-ground testing of in-space body injection into geodesic motion. Review of Scientific Instruments, 2011, 82, 125107.	1.3	17
90	Post-perihelion photometry of dust grains in the coma of 67P Churyumov–Gerasimenko. Monthly Notices of the Royal Astronomical Society, 2017, 469, S195-S203.	4.4	17

#	Article	IF	CITATIONS
91	Assisted Gait Phase Estimation Through an Embedded Depth Camera Using Modified Random Forest Algorithm Classification. IEEE Sensors Journal, 2020, 20, 3343-3355.	4.7	17
92	AUSILIA: Assisted unit for simulating independent living activities. , 2016, , .		16
93	Beta synchrony in the cortico-basal ganglia network during regulation of force control on and off dopamine. Neurobiology of Disease, 2019, 127, 253-263.	4.4	16
94	Multilevel assessment of mental stress via network physiology paradigm using consumer wearable devices. Journal of Ambient Intelligence and Humanized Computing, 2021, 12, 4409-4418.	4.9	16
95	The Agilkia boulders/pebbles size–frequency distributions: OSIRIS and ROLIS joint observations of 67P surface. Monthly Notices of the Royal Astronomical Society, 2016, 462, S242-S252.	4.4	15
96	Exposed bright features on the comet 67P/Churyumov–Gerasimenko: distribution and evolution. Astronomy and Astrophysics, 2018, 613, A36.	5.1	15
97	Surface evolution of the Anhur region on comet 67P/Churyumov-Gerasimenko from high-resolution OSIRIS images. Astronomy and Astrophysics, 2019, 630, A13.	5.1	15
98	A Unified Framework for Uncertainty, Compatibility Analysis, and Data Fusion for Multi-Stereo 3-D Shape Estimation. IEEE Transactions on Instrumentation and Measurement, 2010, 59, 2834-2842.	4.7	14
99	Possible interpretation of the precession of comet 67P/Churyumov-Gerasimenko. Astronomy and Astrophysics, 2016, 590, A46.	5.1	14
100	Uncertainty Evaluation in Two-Dimensional Indirect Measurement by Evidence and Probability Theories. IEEE Transactions on Instrumentation and Measurement, 2010, 59, 2816-2824.	4.7	13
101	Augmented Reality to Enhance the Clinician's Observation During Assessment of Daily Living Activities. Lecture Notes in Computer Science, 2017, , 3-21.	1.3	13
102	Long-term monitoring of comet 67P/Churyumov–Gerasimenko's jets with OSIRIS onboard Rosetta. Monthly Notices of the Royal Astronomical Society, 2017, 469, S380-S385.	4.4	13
103	Search for satellites near comet 67P/Churyumov-Gerasimenko using Rosetta/OSIRIS images. Astronomy and Astrophysics, 2015, 583, A19.	5.1	13
104	Observations of Comet 9P/Tempel 1 around the Deep Impact event by the OSIRIS cameras onboard Rosetta. Icarus, 2007, 191, 241-257.	2.5	12
105	Measurement of the momentum transferred between contacting bodies during the LISA test-mass release phase—uncertainty estimation. Measurement Science and Technology, 2009, 20, 055101.	2.6	12
106	Modelling of the outburst on 2015 July 29 observed with OSIRIS cameras in the Southern hemisphere of comet 67P/Churyumov–Gerasimenko. Monthly Notices of the Royal Astronomical Society, 2017, 469, S178-S185.	4.4	12
107	Characterization of dust aggregates in the vicinity of the Rosetta spacecraft. Monthly Notices of the Royal Astronomical Society, 2017, 469, S312-S320.	4.4	12
108	Opposition effect on comet 67P/Churyumov-Gerasimenko using Rosetta-OSIRIS images. Astronomy and Astrophysics, 2017, 599, A11.	5.1	11

#	Article	IF	CITATIONS
109	Multivariate statistical analysis of OSIRIS/Rosetta spectrophotometric data of comet 67P/Churyumov-Gerasimenko. Astronomy and Astrophysics, 2017, 600, A115.	5.1	11
110	Photometry of dust grains of comet 67P and connection with nucleus regions. Astronomy and Astrophysics, 2016, 588, A59.	5.1	10
111	Kinect-Based Micro-Behavior Sensing System for Learning the Smart Assistance with Human Subjects Inside Their Homes. , 2018, , .		9
112	Multidisciplinary analysis of the Hapi region located on Comet 67P/Churyumov–Gerasimenko. Monthly Notices of the Royal Astronomical Society, 2019, 485, 2139-2154.	4.4	9
113	Diurnal variation of dust and gas production in comet 67P/Churyumov-Gerasimenko at the inbound equinox as seen by OSIRIS and VIRTIS-M on board Rosetta. Astronomy and Astrophysics, 2019, 630, A23.	5.1	9
114	Seasonal variations in source regions of the dust jets on comet 67P/Churyumov-Gerasimenko. Astronomy and Astrophysics, 2019, 630, A17.	5.1	9
115	The Rockyâ€Like Behavior of Cometary Landslides on 67P/Churyumovâ€Gerasimenko. Geophysical Research Letters, 2019, 46, 14336-14346.	4.0	9
116	An object localization and reaching method for wheeled mobile robots using laser rangefinder. , 2008, , .		8
117	Characterization of OSIRIS NAC filters for the interpretation of multispectral data of comet 67P/Churyumov-Gerasimenko. Astronomy and Astrophysics, 2015, 583, A45.	5.1	8
118	Distance determination method of dust particles using Rosetta OSIRIS NAC and WAC data. Planetary and Space Science, 2017, 143, 256-264.	1.7	8
119	Geomorphological and spectrophotometric analysis of Seth's circular niches on comet 67P/Churyumov–Gerasimenko using OSIRIS images. Monthly Notices of the Royal Astronomical Society, 2017, 469, S238-S251.	4.4	8
120	The influence of measurements and feature types in automatic micro-behavior recognition in meal preparation. IEEE Instrumentation and Measurement Magazine, 2018, 21, 10-14.	1.6	8
121	An Augmented Reality Virtual Assistant to Help Mild Cognitive Impaired Users in Cooking a System Able to Recognize the User Status and Personalize the Support. , 2018, , .		8
122	Assessment of Mental Stress Through the Analysis of Physiological Signals Acquired From Wearable Devices. Lecture Notes in Electrical Engineering, 2019, , 243-256.	0.4	8
123	Sigma- <i>z</i> random forest, classification and confidence. Measurement Science and Technology, 2019, 30, 025002.	2.6	8
124	Real-Time Uncertainty Estimation of Autonomous Guided Vehicle Trajectory Taking Into Account Correlated and Uncorrelated Effects. IEEE Transactions on Instrumentation and Measurement, 2007, 56, 696-703.	4.7	7
125	Shape measurement system for single point incremental forming (SPIF) manufacts by using trinocular vision and random pattern. Measurement Science and Technology, 2012, 23, 115402.	2.6	7
126	Garment-based motion capture (GaMoCap): high-density capture of human shape in motion. Machine Vision and Applications, 2015, 26, 955-973.	2.7	7

#	Article	IF	CITATIONS
127	Thermophysics of fractures on comet 67P/Churyumov-Gerasimenko. Astronomy and Astrophysics, 2017, 608, A121.	5.1	7
128	Pronounced morphological changes in a southern active zone on comet 67P/Churyumov-Gerasimenko. Astronomy and Astrophysics, 2019, 630, A8.	5.1	7
129	RoboEye, an Efficient, Reliable and Safe Semi-Autonomous Gaze Driven Wheelchair for Domestic Use. Technologies, 2021, 9, 16.	5.1	7
130	Pallet Pose Estimation with LIDAR and Vision for Autonomous Forklifts. IFAC Postprint Volumes IPPV / International Federation of Automatic Control, 2009, 42, 612-617.	0.4	6
131	Validation of MEMS acceleration measurements for seismic monitoring with LVDT and vision system. , 2012, , .		6
132	Development of Innovative HMI Strategies for Eye Controlled Wheelchairs in Virtual Reality. Lecture Notes in Computer Science, 2016, , 358-377.	1.3	6
133	The backscattering ratio of comet 67P/Churyumov-Gerasimenko dust coma as seen by OSIRIS onboard Rosetta. Monthly Notices of the Royal Astronomical Society, 0, , .	4.4	6
134	Rosetta/OSIRIS observations of the 67P nucleus during the April 2016 flyby: high-resolution spectrophotometry. Astronomy and Astrophysics, 2019, 630, A9.	5.1	6
135	Development of a reduced size unmanned car. , 2008, , .		5
136	Self-Weighted Multilateration for Indoor Positioning Systems. Sensors, 2019, 19, 872.	3.8	5
137	Augmented Robotics for Electronic Wheelchair to Enhance Mobility in Domestic Environment. Lecture Notes in Computer Science, 2017, , 22-32.	1.3	5
138	Four path following controllers for rhombic like vehicles. , 2013, , .		4
139	Quantitative analysis of isolated boulder fields on comet 67P/Churyumov-Gerasimenko. Astronomy and Astrophysics, 2019, 630, A15.	5.1	4
140	The Human Being at the Center of Smart Factories Thanks to Augmented Reality. , 2019, , .		4
141	The Feasibility of Augmented Reality as a Support Tool for Motor Rehabilitation. Lecture Notes in Computer Science, 2020, , 165-173.	1.3	4
142	Human identification and tracking using ultra-wideband-vision data fusion in unstructured environments. Acta IMEKO (2012), 2021, 10, 124.	0.7	4
143	Uncertainty evaluation of 2D vehicle position measurement by probability and theory of evidence approaches. , 2008, , .		3
144	Uncertainty analysis for multi-stereo 3d shape estimation. , 2009, , .		3

Uncertainty analysis for multi-stereo 3d shape estimation. , 2009, , . 144

#	Article	IF	CITATIONS
145	Augmented Virtualized Observation of Hidden Physical Quantities in Occupational Therapy. , 2018, , .		3
146	Minimally Invasive Assessment of Mental Stress based on Wearable Wireless Physiological Sensors and Multivariate Biosignal Processing. , 2019, , .		3
147	Augmented Reality to Enhance the Clinical Eye: The Improvement of ADL Evaluation by Mean of a Sensors Based Observation. Lecture Notes in Computer Science, 2019, , 291-296.	1.3	3
148	Stepping over Obstacles with Augmented Reality based on Visual Exproprioception. , 2020, , .		3
149	Test-Mass Release Phase Ground Testing for the LISA Pathfinder Mission. AIP Conference Proceedings, 2006, , .	0.4	2
150	Inter-eye: Interactive error compensation for eye-tracking devices. AIP Conference Proceedings, 2016, , .	0.4	2
151	Spectrophotometric variegation of the layering in comet 67P/Churyumov-Gerasimenko as seen by OSIRIS. Astronomy and Astrophysics, 2019, 630, A16.	5.1	2
152	Technological Infrastructure Supports New Paradigm of Care for Healthy Aging: The Living Lab Ausilia. Lecture Notes in Electrical Engineering, 2021, , 85-99.	0.4	2
153	Reactive Simulation for Real-Time Obstacle Avoidance. , 2008, , 249-261.		2
154	Monte Carlo-based 3D surface point cloud volume estimation by exploding local cubes faces. Acta IMEKO (2012), 2022, 11, 1.	0.7	2
155	Real-Time Uncertainty Estimation of Odometric Trajectory as a Function of the Actual Manoeuvres of Autonomous Guided Vehicles. , 0, , .		1
156	A New Direct Deformation Measurement System to Enhance Positioning Accuracy of Machine Tools. , 2006, , 51.		1
157	Adaptive-randomised self-calibration of electro-mechanical shutters for space imaging. Mechanical Systems and Signal Processing, 2006, 20, 2305-2320.	8.0	1
158	Description and application of a new method for uncertainty evaluation in two-dimensional indirect measurement. , 2009, , .		1
159	A joint force-position measurement system for neuromotor performances assessment. , 2011, , .		1
160	The use of INTER-EYE for 3D eye-tracking systematic error compensation. , 2016, , .		1
161	Eye tracker uncertainty analysis and modelling in real time. Journal of Physics: Conference Series, 2017, 778, 012002.	0.4	1
162	Phase-curve analysis of comet 67P/Churyumov-Gerasimenko at small phase angles. Astronomy and Astrophysics, 2019, 630, A11.	5.1	1

#	Article	IF	CITATIONS
163	UPPER LIMB LOADS DURING ROBOTIC ASSISTED GAIT: A MEASURING SYSTEM TO GUIDE TRAINING. , 2017, , .		1
164	Wheelchair driving strategies: A comparison between standard joystick and gaze-based control. Assistive Technology, 2023, 35, 180-192.	2.0	1
165	Tensile strength of 67P/Churyumov-Gerasimenko nucleus material from overhangs (<i>Corrigendum</i>). Astronomy and Astrophysics, 2018, 614, C2.	5.1	О
166	Reliability assessment on human activity recognition. , 2019, , .		0
167	A Method for Asteroids 3D Surface Reconstruction from Close Approach Distances. Lecture Notes in Computer Science, 2011, , 21-30.	1.3	Ο
168	Preliminary calibration results of the wide angle camera of the imaging instrument OSIRIS for the Rosetta mission. , 2017, , .		0
169	Position Measurement and Uncertainty Analysis for the Shutter Mechanism Mounted on the Rosetta Mission. , 2018, , .		Ο
170	Object Pose Detection to Enable 3D Interaction from 2D Equirectangular Images in Mixed Reality Educational Settings. Applied Sciences (Switzerland), 2022, 12, 5309.	2.5	0
171	Stabilization of spherical videos based on feature uncertainty. Visual Computer, 0, , .	3.5	0